PEER REVIEW, Vol. 5, Nº 22, 2023
DOI: 10.53660/1207.prw2714
ISSN: 1541-1389

Investigation of microstructure and hardness of WC-Co modified by graphene oxide deposited by HVOF

Investigação da microestrutura e dureza do WC-Co Modificado por óxido de grafeno depositado por HVOF

Celmo Hudson Reis de Paula
ORCID: https://orcid.org/0000-0001-9918-7087
Federal University of Rio Grande do Norte, Brazil
E-mail: celmohudsonr@gmail.com
Meysam Mashhadikarimi
ORCID: https://orcid.org/0000-0003-1449-3654
Federal University of Rio Grande do Norte, Brazil
E-mail: meysam.mashhadikarimi@ufrn.br
Anderson Costa Marques
ORCID: https://orcid.org/0000-0002-8846-658X
Federal University of Rio Grande do Norte, Brazil
E-mail: andersoncosta.m01@gmail.com
Ramon Sigifredo Cortes
ORCID: https://orcid.org/0000-0003-2392-9341
University of Paraná, Brazil
E-mail: ramon@ufpr.br
Rullian Ferreira Pinheiro
ORCID: https://orcid.org/0000-0001-6890-3984
University of Paraná, Brazil
E-mail: rullianpinheiro@hotmail.com
José Heriberto Oliveira do Nascimento
ORCID: https://orcid.org/0000-0001-6804-2854
Federal University of Rio Grande do Norte, Brazil
E-mail: heriberoliver@hotmail.com
Rubens Maribondo do Nascimento
ORCID: https://orcid.org/0000-0001-9094-0044
Federal University of Rio Grande do Norte, Brazil
E-mail: rubens.maribondo@gmail.com

Resumo

O processo de aspersão por combustível de oxigênio de alta velocidade (HVOF) foi utilizado para fabricar carboneto de tungstênio - 12% em peso de cobalto (WC-12Co) com diferentes teores de óxido de grafeno (GO) (0, 0,5, 0,75 e 1% em peso). Foram utilizadas as técnicas de DRX, MEV-FEG, Raman e microdureza Vickers para caracterizar os pós e os revestimentos aplicados. Os resultados experimentais revelaram que os valores de microdureza aumentaram em 19,6% na presença de GO, demonstrando que o GO melhora as propriedades mecânicas do revestimento.

Palavras-chave: Óxido de grafeno; Aspersão térmica; HVOF; Revestimento, WC-Co

Recebido: 10/09/2023 | Aceito: 12/10/2023 | Publicado: 21/10/2023

ABSTRACT

High-velocity oxygen fuel (HVOF) spray process was employed to fabricate tungsten carbide – 12 wt% of cobalt (WC-12Co) with different graphene oxide (GO) contents (0, 0.5, 0.75 and 1 wt%). XRD, SEM-FEG, Raman and Vickers microhardness were used to characterize the powders and applied coatings. The experimental results were revealed that the microhardness values increased by 19,6% with the presence of GO, demonstrating that GO enhances the mechanical properties of the coating.

Keywords : Graphene oxide; Thermal spray; HVOF; Coating, WC-Co

INTRODUCTION

Corrosion and wear caused by degrading work environments have long been significant issues in the oil and gas sectors, resulting in a revenue reduction owing to the high cost of spare component replacements. In the United States, the yearly cost of dealing with corrosion-related issues is approximately 170 billion dollars, with the oil and gas sectors accounting for more than half of this value (IJAOLA; FARAYIBI; ASMATULU, 2020).

As a result, engineering process advancements to change the surface characteristics of metallic materials, such as coating deposition by thermal spraying to increase the surface wearing resistance qualities of materials, have been incredibly common in industries (ZHENG; LIU; QIN; CHEN *et al.*, 2017). Surface engineering has the advantage of using small amounts of pricey materials to strengthen a large volume of substrate (DING; WEI; QUN, 2011), making it a particularly cost-benefit relevant technique for companies.

Cemented carbide-based coatings are employed in the oil and gas, automotive, aeronautics, and mining sectors due to their great wear resistance (DERELIZADE; VENTURI; WELLMAN; KHOLOBYSOV *et al.*, 2021). This attribute gives a tremendous opportunity to extend the life of industry assets, lowering costs and decreasing production downtime (PICAS; PUNSET; RUPÉREZ; MENARGUES *et al.*, 2019).

During working hours in chemically harsh conditions, these materials are susceptible to oxidation, chemical corrosion, and erosion with physical wear processes. When these coatings are corroded, the surface becomes more susceptible to wear, lowering their life span (ZHANG; ZHOU; LIU; LI *et al.*, 2019).

Adding nanoparticles such as graphene, carbon nanotubes, carbides, and alumina to a WC-based coating improves its resistance to wear and corrosion (MYALSKA; MICHALSKA; MOSKAL; SZYMAŃSKI, 2017; PRAKRATHI; BALASUBRAMANYA; KUMAR, 2021; RODRÍGUEZ; GIL; CAMERO; FRÉTY *et al.*, 2014; SU; ZOU; SUN, 2020; ZHANG; ZHANG; DING, 2022). This homogenous mixture produces a bimodal distribution in the material, resulting in hardmetal on a micrometrical scale with nanoparticulate powder dispersion (MYALSKA; LUSVARGHI; BOLELLI; SASSATELLI *et al.*, 2019).

Because of their unique features such as impermeability, hydrophobicity, chemical inertia, and thermal stability, carbon-based materials have been studied as reinforcement coatings (CHAUHAN; QURAISHI; ANSARI; SALEH, 2020; LI; SONG; GONG; MO *et al.*, 2021; LIU; LIU; ZHANG; CHEN *et al.*, 2022; SUN; HUANG; ZHAO, 2021; SUN; ZHAO, 2018). Furthermore, as a possible high-performance solid lubricant, graphene promotes outstanding lubrication performance and wear resistance (CLAVERÍA; ELDUQUE; LOSTALÉ; FERNÁNDEZ *et al.*, 2019; LIU; LIU; ZHANG; CHEN *et al.*, 2022; QIN, 2020; TABANDEH-KHORSHID; OMRANI; MENEZES; ROHATGI, 2016).

Thus, this work aims to investigate the variation of GO content in the microstructure, microhardness, and the corrosion behaviour of WC-12wt.%Co-based coating, sprayed by HVOF.

MATERIALS AND METHODS

The basis material of the coating was conventional WC-12wt.% Co powder made by the business XTC Golden Egret (Luoyang, China), with a particle size of 15-45 μm. As reinforcing materials, GO sheets produced by the Federal University of Rio Grande do Norte (Natal, Brazil) using the modified Hummer's technique (MARCANO; KOSYNKIN; BERLIN; SINITSKII *et al.*, 2010) (number of sheets 5, thickness 4 A).

The powders were mixed for 6 h with 90 rpm angular speed in a jar mill with acetone in 4 distinct compositions, as shown in table 1. There were no frictional methods applied. As a substrate, 1020 steel plates with a thickness of 10 mm were utilized. All of the compositions were sprayed with a Diamond Jet DJ Gun from SULZER METCO utilizing the high-speed oxy-fuel (HVOF) technology. Table 2 shows the parameters that were used.

Table 1 – Samples composition

Nomenclature	Composition
C1	WC-12Co
C2	WC-12Co + 0.5%GO
C3	WC-12Co + 0.75%GO
C4	WC-12Co + 1%GO

Source: Prepared by the authors

Table 2 – Sprinkler parameters

Parameter name	Parameter Range
Preheating (°C)	150
Distance (mm)	280
Feed Rate (g/min)	40
Flow N2 (ft/h)	28
Pressure (psi)	140
Number of rounds	4
Number of samples	10

Source: Prepared by the authors

A scanning electron microscope with a field emission gun (SEM-FEG) of the Zeiss model, Auriga brand, was used to study the microstructures of the powders and coatings (cross-section).

The Raman spectroscopy method was used in the coating to confirm the retention of GO in the structure following thermal spraying. The Raman equipment utilized was a Horiba LabRam HR Evolution with a wavelength of 532 nm and an objective lens of 50×.

A SHIMADZU X-ray diffractogram, model XRD – 7000 using radiation of Cu at 40 kV and 30 mA to confirm the crystalline phases. The diffraction patterns were collected in an angular range 2θ = 30-90°, with a step size of 0.05° and a speed of 2°/min. The analysis of the diffractograms will be carried with different softwares. PANalytical X'pert Data collector 2.2i for measurement and the refinement of the samples will be obtained from the Rietveld method using the MAUD software (version 2.26), to determine the lattice parameters and the quantification of phases.

The coating's Vickers microhardness was measured using a microhardness meter of the Future-Tech brand, model FM-810, in accordance with the ASTM-E304 standard (ASTM, 2012) . On the previously polished cross-sectional region of each coating, a total of 5 indentations were established. A HV0.3 and the dwell time was equal to 10s.

RESULTS AND DISCUSSION

Figure 1 shows the morphology of the WC-Co powder employed in this study, which has spheroidal form and particle sizes between 15 and 45 µm. Figure 2 also illustrated the morphologic characteristics of the GO sheets.

Figure 1 - SEM Morphology of P-WC at different magnifications

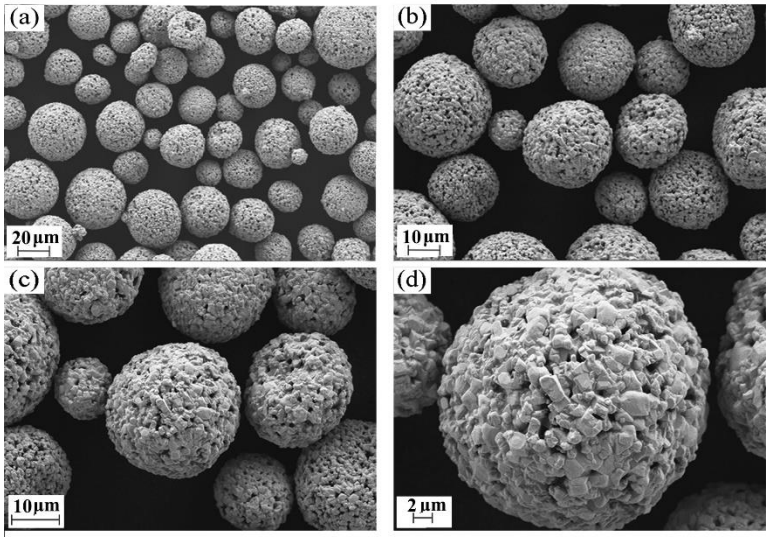

Source: Prepared by the authors

Figure 2 - SEM Morphology of P-GO at different magnifications.

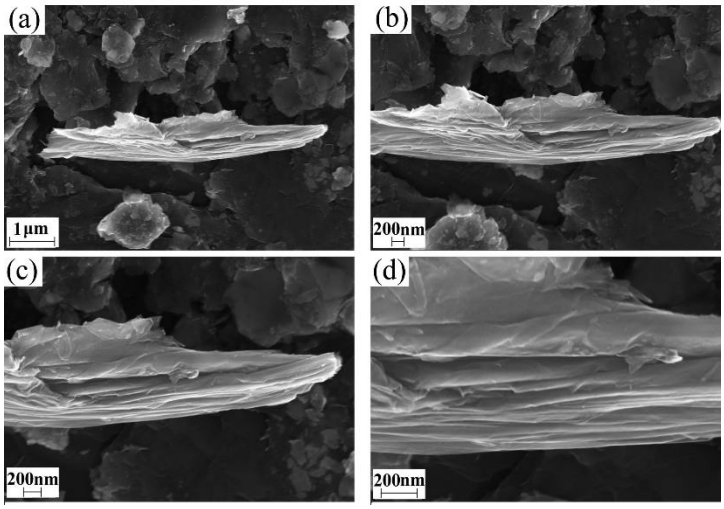

The micrograph in Figure 3 corresponds to the compositions mixed by the mill for 6 hours. The milling procedure did not change the shape of the particles, allowing them to remain spheroidal. Only the adhesion between GO and WC-Co occurred, resulting in WC-Co spheres wrapped in GO sheets (see arrows in Fig. 3a, b, c, d, e, f), with an intimate mixing of the components. Such an effect was expected since the mechanical mixing took place in a ballless mill to minimize impact deformation of the WC-Co particles. - SEM also revealed no obvious agglomerations.

Figure 3 - SEM micrograph of the mixed feeding powders: C2 (a,b), C3 (c,d) and C4 (e,f).

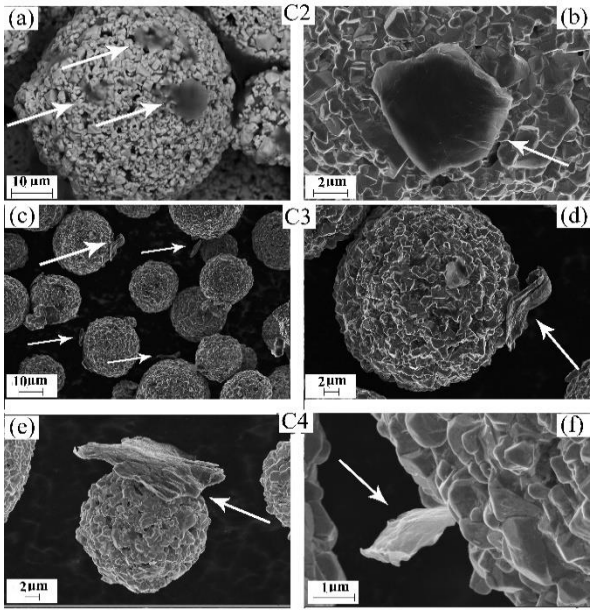

Source: Prepared by the authors

The polished cross-section of the coating obtained using HVOF Thermal spray of the 3 proposed compositions with GO is shown in Figure 4. The image shows the thickness of the sprayed layers, the interface between the substrate and the coating, and whether faults are present. This indicates that there were no discontinuities in any composition at the contact between the substrate and the coating.

Figure 4 - SEM of the cross-sectional area of the coatings: C2 (a,b), C3 (c,d), C4 (e,f).

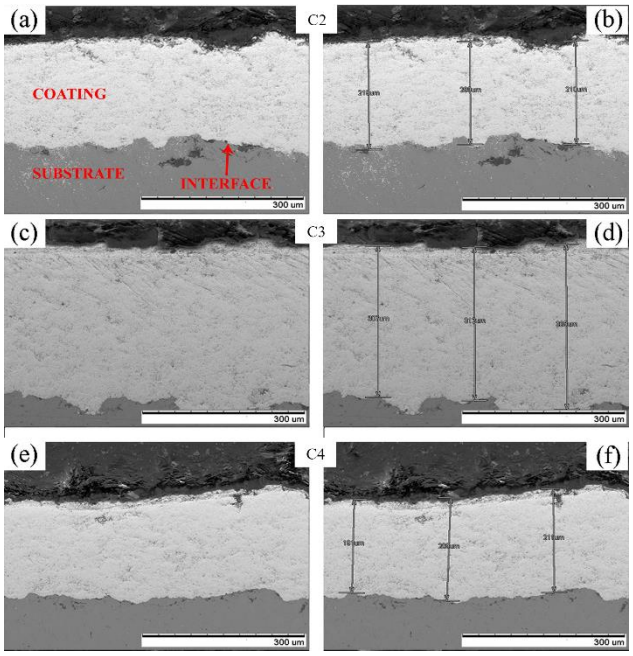

Source: Prepared by the authors

Figure 5 illustrates the Raman spectroscopy of GO sprayed coating. Characteristic bands D and G were found at 1350 cm-1 and 1580 cm-1, respectively. The D-band represents structural defects caused by oxygenation group fixing in the basal carbon plane, while the G-band indicates sp2 hybridization carbon networks (SINGH; KUMAR; SINGH, 2016). The G band is a GO characteristic with a higher intensity than the D band (AIN; HAQ; ALSHAMMARI; AL-MUTLAQ *et al.*, 2019; AKSU; ŞAHIN; ALANYALıOĞLU, 2022). It should be noticed that the GO was still present in the coating after HVOF.

Figure 5 - Raman GO coating

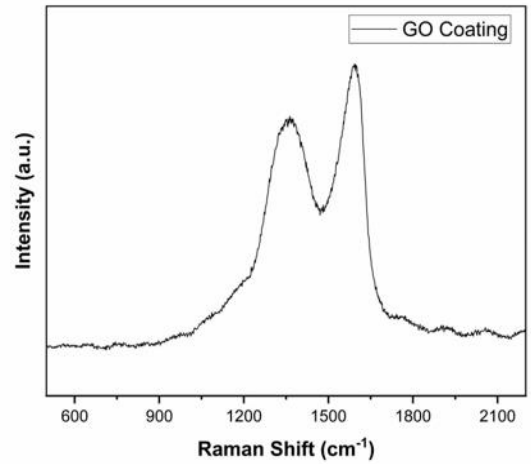

Source: Prepared by the authors

The refined XRD patterns of the compositions C1, C2, C3 and C4 obtained by HVOF are shown in Figure 6. As noted, all peaks are characteristic of WC (WC – type structure, with lattice parameter a = 2.9065 Å, ICSD n◦ 15406, space group P-6m 2(187)), W (bcc#W– type structure, with lattice parameter a = 3.16475(20) Å, ICSD n◦ 43421, space group Im-3m(229)), Co3W3C (η-Carbide#Fe3W3C type structure, with lattice parameter 11,112 Å), ICSD n◦ 166747, space group F d-3 m S(227)), CoO (Sphalerite#ZnS(cF8) type group, with lattice parameter a = 4.55 Å, ICSD n◦ 29082, space group F-43 m(216)), W2C (W2C(hP3) type structure, with lattice parameter a = 2.992 Å, ICSD n◦ 77567, space group P63/mm c (194)), Co6W6C (η-Carbide#Fe6W6C type structure, with lattice parameter a = 10.90 Å, ICSD n◦ 198816, space group Fd-3mZ(227)).

The WC phase remained dominant in all compositions after spraying, with undesirable phases of W2C and W also forming. According to some studies (CHEN; GOU; TU; LIU, 2009; GUILEMANY; DOSTA; MIGUEL, 2006; HE; SCHOENUNG, 2002; KEAR; SKANDAN; SADANGI, 2001; STEWART; SHIPWAY; MCCARTNEY, 2000; YANG; SENDA; OHMORI, 2003), these phases are formed by the high temperatures and oxygen present in the spraying process, as a result, the decomposition products might dissolve in the Co metal matrix to form complex carbide CoxWyC. These decarbonization mechanism have been discussed previously (GUILEMANY; DOSTA; MIGUEL, 2006; HE; SCHOENUNG, 2002; KEAR; SKANDAN; SADANGI, 2001; STEWART; SHIPWAY; MCCARTNEY, 2000; YANG; SENDA; OHMORI, 2003). The presence of GO had no discernible effect on the diffractogram peaks and quantifications phases.

Figure 6 - Refined XRD patterns of C1, C2, C3 and C4 obtained by HVOF

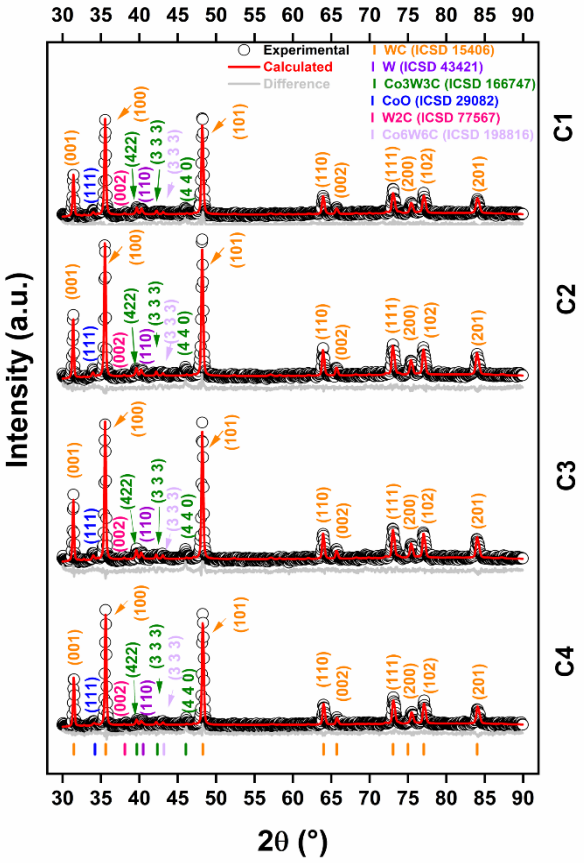

Source: Prepared by the authors

The microhardness values of the coatings of each composition are shown in Figure 7. The addition of GO to the coating increased the material's hardness of up to 17.6%. Nano particles are normally very hard particles, in addition to the special mechanical characteristics of GO (ALGUL; TOKUR; OZCAN; UYSAL *et al.*, 2015), the load is transferred to the GO during the indentation, giving stronger resistance to plastic deformation when is applied load on the material (DRAPER; YEE; PEDRANA; KYI *et al.*, 2022). Furthermore, the bridge formed by GO between the sprayed WC-Co particles limits the particles' relative motion (HE; MA; WANG; YONG *et al.*, 2016). As a result, the triple effect tends to improve the material's hardness.

Figure 7 - Vickers microhardness values for each composition.

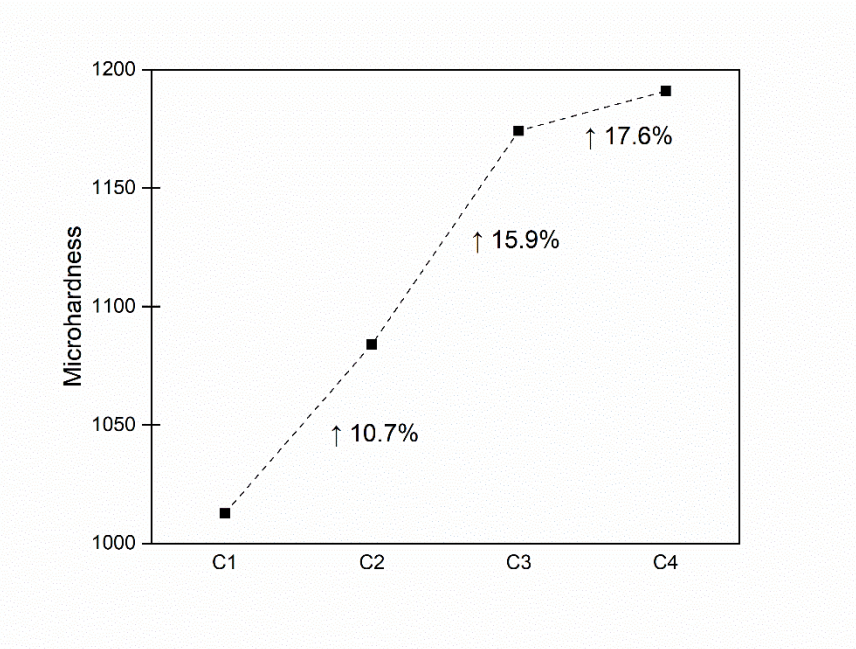

Source: Prepared by the authors

CONCLUSIONS

In this study, the commercial cermet powder WC-12Co was sprayed by HVOF with 4 different concentrations of GO (0, 0.5, 0.75 and 1 wt%). The microscopic morphology, chemical composition, phases and the microhardness of WC-Co/GO were investigated by SEM, X-ray diffraction techniques, raman spectroscopy and microhardness test. The results of this study are as bellow.

(1) The mixing of GO and WC-Co in a jar mill without frictional methods was successful confirmed by SEM.

(2) The GO was successfully incorporated in the coating confirmed by raman spectroscopy carried out on the cross-section of the coating, so, HVOF can be employed to prepare coatings with nanomaterials.

(3) The diffractogram peaks and quantifications phases were not affected by the presence of GO. The HVOF coatings manly consists of WC, CoO, W_2C, W. There also exist Co_xW_yC, amorphous phases in the coating.

(4) The microhardness test carried out on the cross-sections of the coatings demonstrated that the addition of GO increased hardness by 19.6%.

REFERENCES

AIN, Q. T.; HAQ, S. H.; ALSHAMMARI, A.; AL-MUTLAQ, M. A. *et al.* The systemic effect of PEG-nGO-induced oxidative stress in vivo in a rodent model. **Beilstein journal of nanotechnology**, 10, n. 1, p. 901-911, 2019.

AKSU, Z.; ŞAHIN, C. H.; ALANYALıOĞLU, M. Fabrication of Janus GO/rGO humidity actuator by one-step electrochemical reduction route. **Sensors and Actuators B: Chemical**, 354, p. 131198, 2022.

ALGUL, H.; TOKUR, M.; OZCAN, S.; UYSAL, M. *et al.* The effect of graphene content and sliding speed on the wear mechanism of nickel–graphene nanocomposites. **Applied Surface Science**, 359, p. 340-348, 2015.

ASTM, A. E384: standard test method for knoop and vickers hardness of materials. **ASTM Stand**, p. 1-43, 2012.

CHAUHAN, D. S.; QURAISHI, M.; ANSARI, K.; SALEH, T. A. Graphene and graphene oxide as new class of materials for corrosion control and protection: Present status and future scenario. **Progress in Organic Coatings**, 147, p. 105741, 2020.

CHEN, H.; GOU, G.; TU, M.; LIU, Y. Characteristics of nano particles and their effect on the formation of nanostructures in air plasma spraying WC–17Co coating. **Surface and Coatings Technology**, 203, n. 13, p. 1785-1789, 2009.

CLAVERÍA, I.; ELDUQUE, D.; LOSTALÉ, A.; FERNÁNDEZ, Á. *et al.* Analysis of self-lubrication enhancement via PA66 strategies: Texturing and nano-reinforcement with ZrO2 and graphene. **Tribology International**, 131, p. 332-342, 2019.

DERELIZADE, K.; VENTURI, F.; WELLMAN, R.; KHOLOBYSOV, A. *et al.* Wear performance of graphene nano platelets incorporated WC-Co coatings deposited by hybrid high velocity oxy fuel thermal spray. **Wear**, 482, p. 203974, 2021.

DING, Z.-X.; WEI, C.; QUN, W. Resistance of cavitation erosion of multimodal WC-12Co coatings sprayed by HVOF. **Transactions of Nonferrous Metals Society of China**, 21, n. 10, p. 2231-2236, 2011.

DRAPER, B.; YEE, W. L.; PEDRANA, A.; KYI, K. P. *et al.* Reducing liver disease-related deaths in the Asia-Pacific: the important role of decentralised and non-specialist led hepatitis C treatment for cirrhotic patients. **The Lancet Regional Health–Western Pacific**, 20, 2022.

GUILEMANY, J.; DOSTA, S.; MIGUEL, J. The enhancement of the properties of WC-Co HVOF coatings through the use of nanostructured and microstructured feedstock powders. **Surface and Coatings Technology**, 201, n. 3-4, p. 1180-1190, 2006.

HE, J.; SCHOENUNG, J. M. Nanostructured coatings. **Materials Science and Engineering: A**, 336, n. 1-2, p. 274-319, 2002.

HE, P.; MA, G.; WANG, H.; YONG, Q. *et al.* Microstructure and mechanical properties of a novel plasma-spray TiO2 coating reinforced by CNTs. **Ceramics International**, 42, n. 11, p. 13319-13325, 2016.

IJAOLA, A. O.; FARAYIBI, P. K.; ASMATULU, E. Superhydrophobic coatings for steel pipeline protection in oil and gas industries: A comprehensive review. **Journal of Natural Gas Science and Engineering**, 83, p. 103544, 2020/11/01/ 2020.

KEAR, B.; SKANDAN, G.; SADANGI, R. Factors controlling decarburization in HVOF sprayed nano-WC/Co hardcoatings. **Scripta Materialia**, 44, n. 8-9, p. 1703-1707, 2001.

LI, M.; SONG, Z.; GONG, M.; MO, D. *et al.* WC+ Co+ graphene platelet composites with improved mechanical, tribological and thermal properties. **Ceramics International**, 47, n. 21, p. 30852-30859, 2021.

LIU, Y.; LIU, X.; ZHANG, X.; CHEN, X. *et al.* Tribological properties and self-lubrication mechanism of in-situ grown graphene reinforced nickel matrix composites in ambient air. **Wear**, 496, p. 204308, 2022.

MARCANO, D. C.; KOSYNKIN, D. V.; BERLIN, J. M.; SINITSKII, A. *et al.* Improved synthesis of graphene oxide. **ACS nano**, 4, n. 8, p. 4806-4814, 2010.

MYALSKA, H.; LUSVARGHI, L.; BOLELLI, G.; SASSATELLI, P. *et al.* Tribological behavior of WC-Co HVAF-sprayed composite coatings modified by nano-sized TiC addition. **Surface and Coatings Technology**, 371, p. 401-416, 2019.

MYALSKA, H.; MICHALSKA, J.; MOSKAL, G.; SZYMAŃSKI, K. Effect of nano-sized TiC powder on microstructure and the corrosion resistance of WC-Co thermal spray coatings. **Surface and Coatings Technology**, 318, p. 270-278, 2017.

PICAS, J.; PUNSET, M.; RUPÉREZ, E.; MENARGUES, S. *et al.* Corrosion mechanism of HVOF thermal sprayed WC-CoCr coatings in acidic chloride media. **Surface and Coatings Technology**, 371, p. 378-388, 2019.

PRAKRATHI, S.; BALASUBRAMANYA, H.; KUMAR, T. A. Influence of carbon nano tube additions on coating characteristics of WC-Co/Cr3C2-NiCr on T12 substrate. **Materials Today: Proceedings**, 46, p. A1-A3, 2021.

QIN, X. Self-lubrication and wear-resistance mechanism of graphene-modified coatings. **Ceramics International**, 46, n. 10, p. 15915-15924, 2020.

RODRÍGUEZ, M.; GIL, L.; CAMERO, S.; FRÉTY, N. *et al*. Effects of the dispersion time on the microstructure and wear resistance of WC/Co-CNTs HVOF sprayed coatings. **Surface and Coatings Technology**, 258, p. 38-48, 2014.

SINGH, R. K.; KUMAR, R.; SINGH, D. P. Graphene oxide: strategies for synthesis, reduction and frontier applications. **Rsc Advances**, 6, n. 69, p. 64993-65011, 2016.

STEWART, D.; SHIPWAY, P.; MCCARTNEY, D. Microstructural evolution in thermally sprayed WC–Co coatings: comparison between nanocomposite and conventional starting powders. **Acta Materialia**, 48, n. 7, p. 1593-1604, 2000.

SU, W.; ZOU, J.; SUN, L. Effects of nano-alumina on mechanical properties and wear resistance of WC-8Co cemented carbide by spark plasma sintering. **International Journal of Refractory Metals and Hard Materials**, 92, p. 105337, 2020.

SUN, J.; HUANG, Z.; ZHAO, J. High-hard and high-tough WC-TiC-Co cemented carbide reinforced with graphene. **Materials Today Communications**, 29, p. 102841, 2021.

SUN, J.; ZHAO, J. Multi-layer graphene reinforced nano-laminated WC-Co composites. **Materials Science and Engineering: A**, 723, p. 1-7, 2018.

TABANDEH-KHORSHID, M.; OMRANI, E.; MENEZES, P. L.; ROHATGI, P. K. Tribological performance of self-lubricating aluminum matrix nanocomposites: role of graphene nanoplatelets. **Engineering science and technology, an international journal**, 19, n. 1, p. 463-469, 2016.

YANG, Q.; SENDA, T.; OHMORI, A. Effect of carbide grain size on microstructure and sliding wear behavior of HVOF-sprayed WC–12% Co coatings. **Wear**, 254, n. 1-2, p. 23-34, 2003.

ZHANG, X.; ZHANG, J.; DING, J. Effect of the additive graphene oxide on tribological properties of WC-Co cemented carbide. **International Journal of Refractory Metals and Hard Materials**, 109, p. 105962, 2022.

ZHANG, X.; ZHOU, J.; LIU, C.; LI, K. *et al.* Effects of Ni addition on mechanical properties and corrosion behaviors of coarse-grained WC-10 (Co, Ni) cemented carbides. **International Journal of Refractory Metals and Hard Materials**, 80, p. 123-129, 2019.

ZHENG, C.; LIU, Y.; QIN, J.; CHEN, C. *et al.* Wear behavior of HVOF sprayed WC coating under water-in-oil fracturing fluid condition. **Tribology International**, 115, p. 28-34, 2017.